Archives of Acoustics Vol. 50, No. 1, pp. 37–45 (2025), https://doi.org/10.24425/aoa.2025.153653

Research Paper

Failure Detection of Powertrain Components in Motor Vehicles Using Vibroacoustic Methods

Balázs József KRISTON, Károly JÁLICS*

Institute of Machine and Product Design, University of Miskolc
Miskolc-Egyetemváros, Hungary

*Corresponding Author e-mail: karoly.jalics@uni-miskolc.hu

(*received February 3, 2024; accepted December 19, 2024; published online March 4, 2025*)

Although noise and vibration measurements are widespread in the machine diagnostics, they are not used in the diagnostics of the powertrain of motor vehicles. Our research aims to investigate the possibilities, advantages, and drawbacks of using noise and vibration diagnostics performed for motor vehicles. In this paper, we attempt to use vibroacoustic signals from a motor vehicle for diagnostic purposes. Ordinary audible malfunctions, for example, misfiring in a passenger car, were artificially created. The differences between the normal and faulty operating conditions were examined to identify evidence of failure in the vibration signal. Primarily, evaluation through Fourier transformation was performed to provide a visual correlation between the fault and the vibration behavior of the car. Detailed conclusions from the measurements and future research plans are discussed.

Keywords: vibration; acoustics; diagnostics; misfire; vehicle; analysis; internal combustion engine; malfunction.

1. Introduction

In the automotive industry, vehicle noise and vibration performance have become an important design parameter, as in other technical fields. Sound quality is one of the main factors that define the product itself, making vibroacoustic control of motor vehicles a key activity for automotive engineers. Furthermore, noise and vibration pollution are regulated by standards, making noise refinement during the predevelopment stage essential to protect users from health problems and other adverse effects. Malfunctions in the car's motor and powertrain can increase overall noise levels, and consequently, reduce good sound quality, leading to a noisier and less refined auditory experience.

One of the most common problems in internal combustion engines (ICEs) is an aged spark plug, which causes weak ignition and results in misfiring. This issue is particularly prevalent in older vehicles and results in reduced fuel efficiency, and potentially causing serious long-term engine damage. Nowadays, misfire detection methods are built-in in every vehicle to comply with environmental protection regulations. Some common detection strategies include measuring cylinder pressure or monitoring speed fluctuation in the crankshaft. Unusual noises from a car can induce stress and feelings of insecurity in drivers. However, this unwanted phenomenon can also be utilized, since the vibration is sensitive to all faults, whereas other physical parameters, such as those monitored by onboard diagnostics system (OBD), are sensitive only to specific faults. This means that monitoring a vehicle's vibration behavior can identify potential failures.

Nevertheless, vibration diagnostics has its limitations, as they depend on the product's complexity, operation mode, and the severity of the fault. Solely relying on the overall sound pressure level (SPL) and averaged vibration spectra does not give a sufficient representation of sound quality. That is why the introduction of psychoacoustic measurements is necessary to gain a more comprehensive insight into human sound perception. On the other hand, psychoacoustic analysis can serve as a diagnostic tool for identifying vehicle malfunctions since experienced mechanics can

often diagnose certain malfunctions in cars by sound alone. For example, at idle speed, a knocking noise from beneath the valve cover may be clearly audible. As the engine's rotational speed increases the noise frequency also increases, which indicates that the valve clearance is too large.

At the Aachen University in Germany (Brecher *et al.*, 2011), a correlation analysis was conducted between gear parameters and psychoacoustic values based on noise measurements from different gear sets. For the research, gear sets with different surface microstructure and pitch deviation were selected. The study found that both the loudness and sharpness of the noise increased with rotational speed. According to the study's findings, roughness proved to be the most valuable parameter for identifying pitch deviation failures in gears. Babu Devasenapati *et al.* (2010) analyzed a four-stroke four-cylinder petrol engine with a misfire problem. For problem identification, they used statistical parameters of vibration signals, such as kurtosis, standard deviation, mean, etc. A decision tree was developed that could extract the most appropriate parameters for failure detection and to classify various ICE misfire problems with 95 % accuracy. Firmino *et al.* (2012) collected vibration and acoustic data from a four-stroke spark ignition engine with a misfire in one cylinder. After performing feature extraction using the fast Fourier transform (FFT) algorithm, the data was used to feed different artificial neural network (ANN) systems in order detect the misfire failure. Both networks demonstrated great results, achieving, accuracy of around 99 % in misfire detection. Delvecchio *et al.* (2018) reviewed the existing state-of-the-art vibroacoustic techniques for diagnosing failures in ICEs, including misfires. According to this study, the most commonly used techniques for ICE malfunctions are joint time-frequency methods. However, these methods are mainly applied to failure detection rather than condition monitoring purposes.

Wojnar and Madej (2009) tested ICEs using vibroacoustic methods and concluded that relying only on the FFT does not deliver sufficient results. They emphasized the advantages of joint time-frequency methods, particularly wavelet analysis. Wojnar and Stanik (2010) compared vibration and acoustic signals for diagnosing car wheel bearings. Their investigation revealed that bearing wear can be determined through vibroacoustic methods. Szabó and Dömötör (2022) also investigated the wheel bearings of a passenger vehicle with vibroacoustic methods, and confirmed that these methods are effective for detecting bearing faults. Wojnar *et al.* (2011) further investigated roller bearing defects, focusing on non-dimensional factors (e.g., impulse factor, crest factor, etc.). Their findings showed that these parameters are sufficient for detecting bearing faults.

Psychoacoustic quantities are not currently involved in detection or monitoring actions. Analysis acoustic data such as SPL obtained from a microphone, is rarely used due to the masking effect of background noise, making it unsuitable for detecting assembly faults. However, joint techniques based on acoustic signals remain useful for capturing and localizing transient events in the time or angular domain, especially when the noise characteristics cover a wide frequency range and originate from different areas of the engine. Such events in ICE could be knocking, misfires, or injection problems. Using these methods, more mechanical events that influence the vibroacoustic behavior of the engine can be captured in a single measurement. On the other hand, misfires produce structure-borne noise, which means that vibration signals are effective for detecting such failures as well. For purely airborne noise, the SPL signal is relevant for: turbocharger, ventilation fan, or exhaust system; however, for mechanical malfunctions, which are structure-borne transmitted, the fault must be in advanced stage to be detectable by acoustic signals. Additionally, the use of transducers allows for targeted examination of sub-components of the ICE, depending on their positioning.

Time domain analysis focuses on observing the shape of the time signal. The information that the time domain contains can be described by the above mentioned statistical single values. While these values are sufficient for detecting malfunctions, they are not effective for localizing failures. To use these values as decision-making criteria in automated diagnostic system, the time signal must be insensible to background noise and should not contain unnecessary information. The signal-to-noise ratio can be maximized by applying frequency band filters to the time signal.

The analysis can also be performed in the frequency domain, where distinct frequency peaks and harmonics correspond to different components. For this purpose, FFT is applied, revealing the frequencies of various events with different energy content. This algorithm is effective only for cyclo-stationary signals, helping to understand the cause of failure and providing reliable information for condition monitoring and diagnostic activities.

As a summary, the authors recommend performing time-frequency analysis when the nature of the fault is impulsive, with the consideration of the level of investigation and computational efforts required. For condition monitoring and failure detection, it is common practice to combine scalar parameters with 2D analysis. In this case, the scalar parameter serves as input for the decision-making algorithm, while the latter is a visual representation for the user. It is important to note that the scalar value must contain all the information stored in the 2D map to ensure accurate diagnostics.

2. Measurement arrangement

Based on our experience and the suggestions of the above-mentioned authors, we performed a test series on a real vehicle. The vehicle was a first-generation Ford Focus passenger car (1998 model; front-wheel drive, 5-speed manual transmission) with a 1.6 liter, 4-cylinder, four-stroke naturally aspirated petrol engine. For data collection, a 4-channel Brüel & Kjaer Photon+ DAQ system was connected through USB to a notebook. The notebook itself was powered by its built-in battery, which helped eliminate the potential interference from the 50 Hz AC mains.

During the measurements, an easy installation of the sensors (accelerometers and a microphone) without dismantling the car was a key requirement. This was based on the general requirement of workshop repair personnel, to avoid excessive disassembly for a simple test. To this end, one uniaxial acceleration sensor was placed on the right front side of the car body, and another was positioned on the connection bolt head between engine block and the gearbox housing (Fig. 1). Additionally, a condenser microphone was placed at the front passenger's head level. The measurements were repeated several times at idle speed with engine speeds of 1000 rpm, 2000 rpm, 3000 rpm, and 4000 rpm, all without load. Furthermore, noise and vibration were measured in accelerated mode under partial open throttle (POT) conditions during a run-up and run-down cycle from 1000 rpm to 5000 rpm and back to 1000 rpm. The length of the run-up and run-down time was controlled by the driver using the gas pedal. During the measurements, the coolant temperature was monitored via the onboard coolant temperature gauge, and it was kept around 90 °C operating temperature during the tests. The acquired raw time signal was later post-processed with the help of Artemis Suite noise evaluation software.

To create a faulty condition in the engine, the operation of one of the four cylinders was eliminated by disabling the ignition in cylinder 1 (on the side of the timing drive). The effect of the misfire was clearly noticeable by ear in the immediate vicinity of the car. The goal of the measurements was to analyze the vibration behavior of the engine in the presence of a misfire fault. Based on this analysis, the potential for detecting and localizing failures should be investigated.

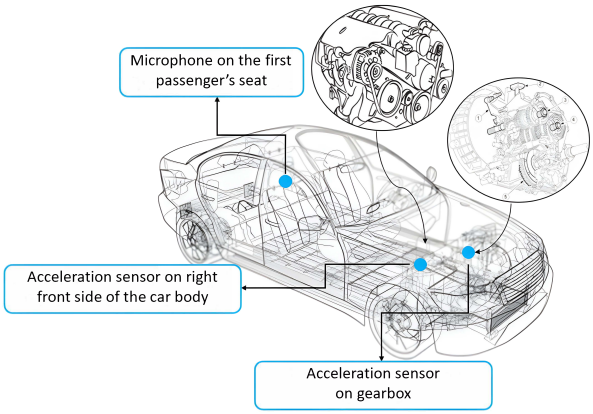

Fig. 1. Sensor positions.

3. Analysis

In the course of the analysis, the raw time signals were post-processed by the FFT algorithm. The purpose of the analysis was to find acoustic patterns which may refer to a malfunctioned part in spectrums and spectrograms.

Initially, the time signals were analyzed. We can state that the microphone signal recorded during the run-up tests provided more promising outputs from a diagnostic perspective, since time domain signal obtained from the microphone's measurement showed better separation (Fig. 3) in sound pressure between healthy (blue) and faulty (red) conditions, compared to the acceleration signal recorded on the gearbox (Fig. 2).

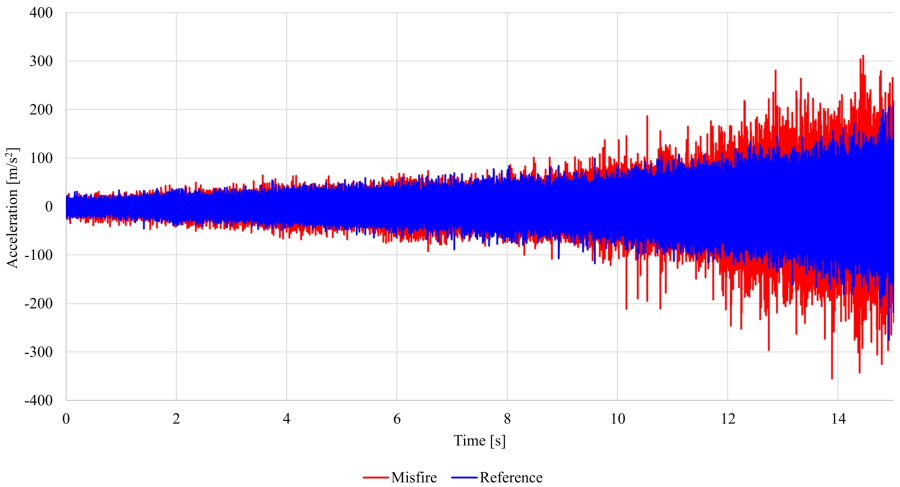

Fig. 2. Gearbox time history at ramp speed of 1500 rpm–4200 rpm.

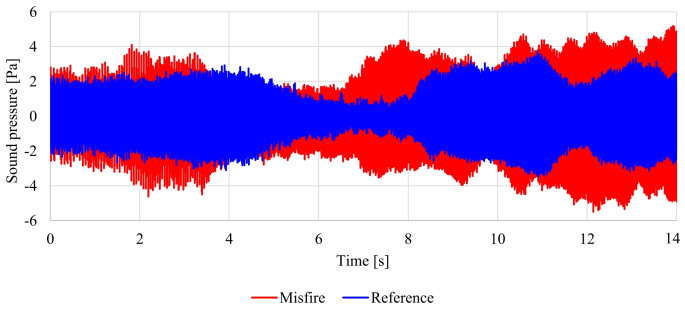

Fig. 3. Microphone time history at ramp speed of 1500 rpm–5000 rpm (POT).

In Fig. 3, the form of the acoustic signal is characterized by the components directed toward the passenger's seat, with different frequency-dependent damping properties. The constant-speed measurements do not seem to be very useful for distinguishing failure modes. However, an interesting effect is observable, especially at higher rotational speed and is evident only in the microphone signal, see Fig. 4.

The shape of the time signal shows a very slow, pure sinusoidal, strong modulation (1.5 Hz–2 Hz). This modulation effect becomes stronger when the engine is misfiring. In our opinion, it is caused by fluctuations in the engine crankshaft's rotational speed, as one can see in Fig. 5. This effect can be explained by different cylinder pressures caused by the misfire. However, it is important to note that combustion engines have a certain speed fluctuation, unlike electric motors. The rpm signal (Fig. 5) was created with an rpm generator, which is a built-in function in the noise evaluator software.

The time interval between the distinct peaks is around 0.0075 seconds, which corresponds to a calculated frequency of 133.33 Hz. This is the ignition frequency at 4000 rpm (Fig. 4), which can be calculated for a 4-stroke internal combustion engine using the following formula:

$$f_{\text{ignition}} = \frac{1}{2} \cdot \frac{\text{rpm}}{60} \cdot \text{cylinders}\ [\text{Hz}], \tag{1}$$

where rpm is the motor crankshaft speed in [1/min], and "cylinders" refers to the number of cylinders (four in this case) and it is divided by two, since two ignition is required to rotate the crankshaft 360° as two cylinders move together at the same time. As the engine construction is fixed, this frequency depends only on the rotational speed.

The motor frequency can be easily calculated as

$$f_{\text{motor}} = \frac{\text{rpm}}{60}\ [\text{Hz}]. \tag{2}$$

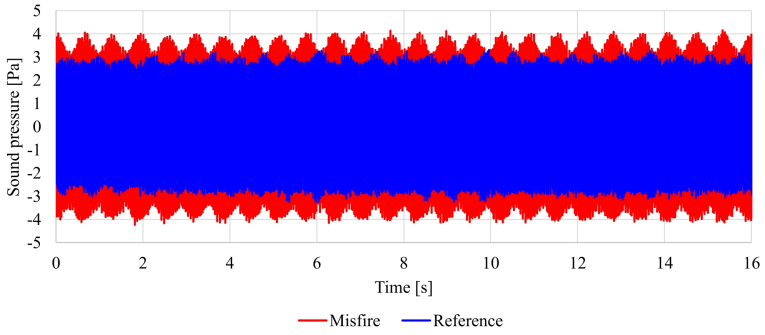

Fig. 4. Microphone time history at constant speed of 4000 rpm.

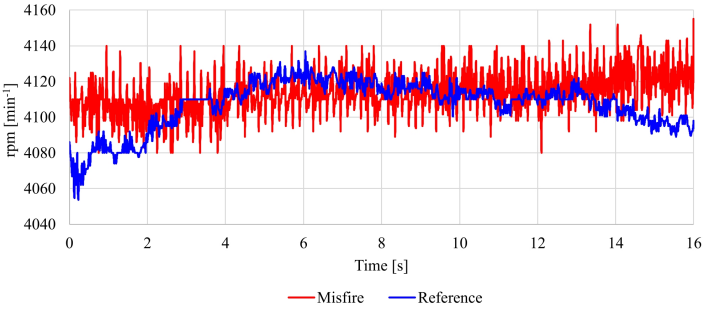

Fig. 5. Rpm curves at constant 4000 rpm derived from the microphone's signal.

The camshaft is connected to the crankshaft through a belt drive. This shaft activates the cylinders' intake and exhaust valves, thus controlling the combustion process. The transmission ratio between the shafts is usually 2:1, which means that the camshaft's rotation speed is half of the motor shaft. Therefore, the camshaft frequency is

$$f_{\text{camshaft}} = \frac{\text{rpm}/2}{60}\ [\text{Hz}], \tag{3}$$

which is the same frequency as the motor 0.5th order. It is observable in the spectrogram of every sensor, but the best representation of the failure can be derived from the microphone's signal. Table 1 presents the first-order fundamental frequencies of the motor at different speeds for comparison in the analysis.

Table 1. Fundamental frequencies of the engine [Hz].

	2000 rpm	3000 rpm	5000 rpm
Crank frequency	33.33	50	83.33
Camshaft frequency	16.66	25	41.66
Ignition frequency	66.67	100	166.67

The ignition frequency is recognizable in both healthy and faulty cases. It means that even under normal conditions, the ignition phenomena characterize the vibration behavior of the motor. Since the time signal during the ramp speed measurements can visualize the problem, single statistical values – such as root mean square (RMS), crest factor, standard deviation, kurtosis, etc., should show a high deviation factor between the two conditions. The RMS value of a given set of discrete data points can be calculated by the following formula:

$$\text{RMS} = \sqrt{\frac{x_1^2 + x_2^2 + x_3^2 + \ldots + x_n^2}{n}}. \tag{4}$$

First, the data points are squared, then the average of all the squared values is taken. After that, the square root of the average is calculated. This process tells us how much energy is contained in the waveform.

The skewness shows the asymmetry of a distribution. If the skewness value is zero, the distribution is symmetrical. A normal distribution has a zero skew. The easiest method to check the skewness is to plot the data on a histogram. If the distribution has right (positive) skew, it means the distribution is shifted to the right relative to the axis of symmetry. Conversely, in the case of left (negative) skew, the distribution is longer on the opposite side (Turney, 2022). The skewness values obtained from the gearbox acceleration sensor and the microphone signal show that the skewness value is negative, while the sensors on the car body yield positive values. The equation for skewness is as follows:

$$\text{Skewness} = \frac{n}{(n-1)(n-2)} \sum \left(\frac{x_i - \overline{x}}{s} \right)^3. \tag{5}$$

The mean value was calculated with the following equation:

$$\text{Mean} = \frac{x_1 + x_2 + x_3 + \ldots + x_n}{n}. \tag{6}$$

The standard deviation is a measure of the spread around the mean value. A low standard deviation means the data are clustered around the mean, while a high standard deviation indicates data are more spread out. The formula used to calculate standard deviation is

$$\text{Standard deviation} = \sqrt{\frac{\sum (x_i - \overline{x})^2}{n-2}}. \tag{7}$$

The peak amplitude derived from the RMS is given by:

$$\text{Peak} = \frac{2}{\sqrt{2}}\text{RMS}. \tag{8}$$

The peak-to-peak amplitude is the difference between the highest positive and the lowest negative amplitude in the waveform:

$$\text{Peak to peak amp.} = \max\{x_i\} - \min\{x_i\}. \tag{9}$$

The crest factor gives the ratio of the peak values to the effective value, showing how prominent the peaks are in the waveform. A crest factor of 1 indicates no peaks, while a higher crest factor indicates peaks. The crest factor is calculated as

$$\text{Crest factor} = \frac{\text{Peak}}{\text{RMS}}. \tag{10}$$

The statistical parameter called kurtosis is a measure of the "peakedness" of a random signal:

$$\text{Kurtosis} = \left\{ \frac{n(n+1)}{(n-1)(n-2)(n-3)} \sum \left(\frac{x_i - \overline{x}}{s} \right)^4 \right\} - \frac{3(n-1)^2}{(n-2)(n-3)}. \tag{11}$$

Unfortunately, the statistical single values of the microphone's time signal do not provide adequate difference between the bad and good conditions (Fig. 6).

The same statement is true for the crest factor values: the failure shows no separation in this parameter compared to the original condition (Fig. 7). However, in certain engine speed ranges (around 2700 rpm and above 4000 rpm) the kurtosis parameter indicates a small deviation between the conditions (Fig. 8).

Nevertheless, the result is not conclusive due to the low distinction of the individual overall values. To better understand the malfunction, joint time-frequency (FFT vs. time) analysis was performed at both constant and ramp speeds. Joint analysis is the representation of series of Fourier transformations over different time periods (or at different rotation speeds),

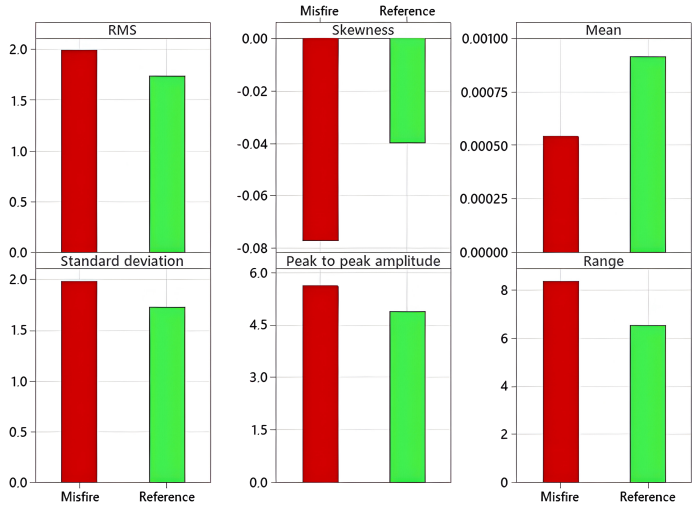

Fig. 6. Time domain statistical single values derived from the microphone's signal on 4000 rpm.

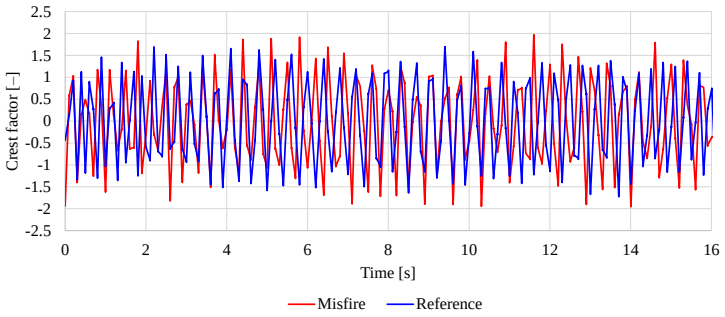

Fig. 7. Crest factor in the function of time derived from the microphone's signal at 4000 rpm.

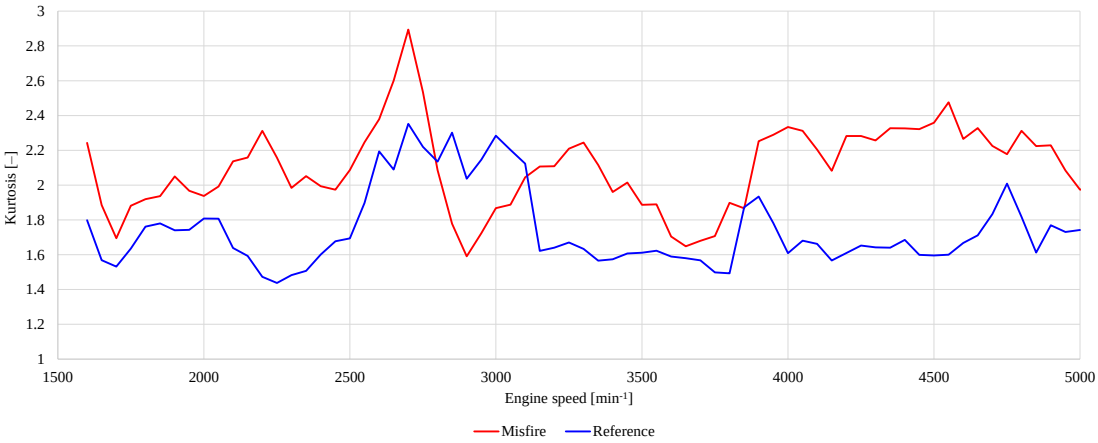

Fig. 8. Kurtosis as a function of engine rotation speed derived from the microphone's ramp signal.

mapping a 1D time domain into a 2D diagram that shows energy (color scale) versus time (x-axis) and frequency (y-axis). This analysis helps to understand how the energy content of frequencies varies over time or as a function of rotation speed. As shown in Fig. 9, it is clear that the sound pressure level increases at specific motor frequencies. The sound pressure at the ignition frequency is a dominant contributor to the overall sound pressure level inside the car, even in healthy condition, where only vibrations below 2000 Hz are significant. The dominance of the ignition frequency is observable at the other measurement points as well. The motor subharmonics create abnormal colormap picture in the case of a misfire issue. Among the topological integer motor frequencies, the motor half-orders (subharmonics) appear with higher energy. This leads to the assumption that the motor 0.5th order (17.58 Hz) causes modulation in the signal. One possible reason

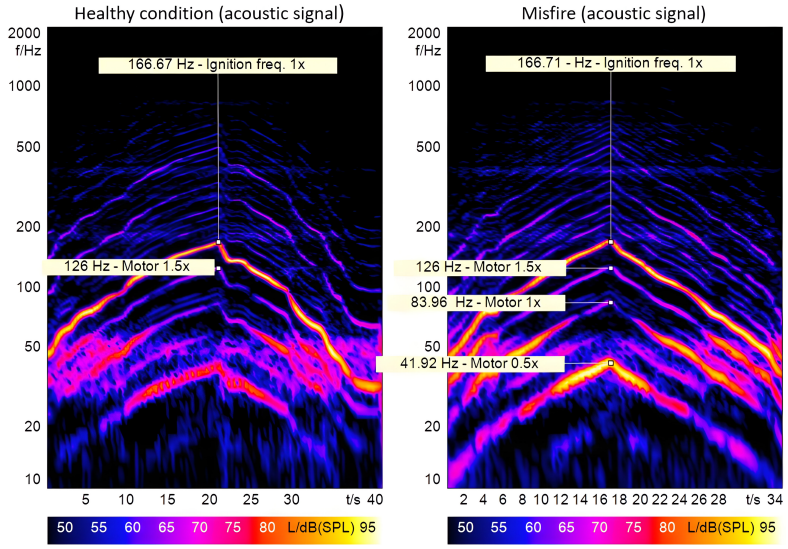

Fig. 9. Microphone spectrogram (10 Hz–2000 Hz) in healthy (left) and faulty (right) conditions during ramp speed (1500 rpm–5000 rpm).

for this is that the engine crankshaft rotation becomes, let us say, more unbalanced due to the misfire in cylinder 1.

Rather than stating that the crankshaft itself is unbalanced, it is more accurate to say that, as a consequence of the misfire, the shaft rotation speed fluctuates, causing uneven running. This hypothesis is supported by Cavina *et al.* (2002), who claim that misfire results in a sudden lack of torque on the crankshaft, leading to damped torsional vibrations at representative frequencies of the engine.

The joint analysis of the acoustic signal made possible to determine the location of the malfunction, as we were able identify frequencies that correspond to the engine crankshaft 0.5th, 1st, 1.5th, 2.5th, and 3rd, as well as other higher-orders. However, one can detect with a high degree of certainty that the failure is coming from the motor by simply listening to the sound of the car. Unfortunately, resonance appears in the joint time-frequency analysis in a similar manner to harmonic frequencies at constant speed. Due to this fact, it is worth considering the spectrogram when the rotation speed varies over time, e.g., in ramped speed measurements.

One can see that there is a resonance at 50 Hz, which increases the sound pressure level of the motor's first order, when it operates between 2400 rpm–3100 rpm (Fig. 10). The order shapes demonstrate how the motor speed changes over time: the motor accelerates over 30 seconds, reaching a maximum speed of 5000 rpm during the run-up, and then slows down to 1500 rpm during the run-down phase. This

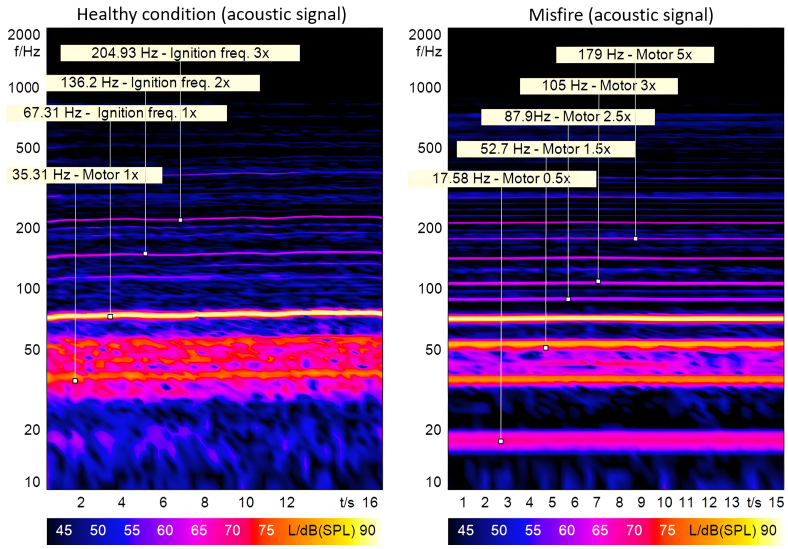

Fig. 10. Microphone spectrogram (10 Hz–2000 Hz) in healthy (left) and faulty (right) conditions at 2000 rpm.

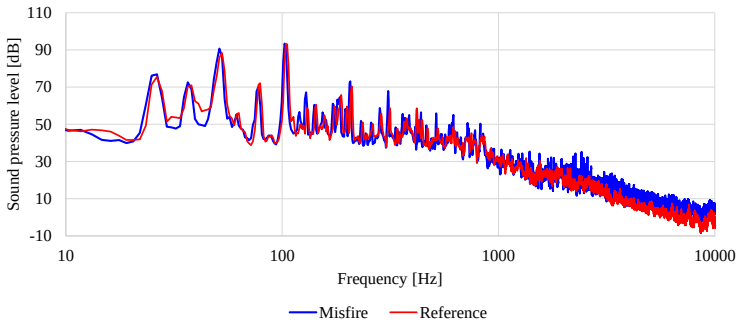

Fig. 11. Microphone's spectrum comparison at 3000 rpm (logarithmic abscissa).

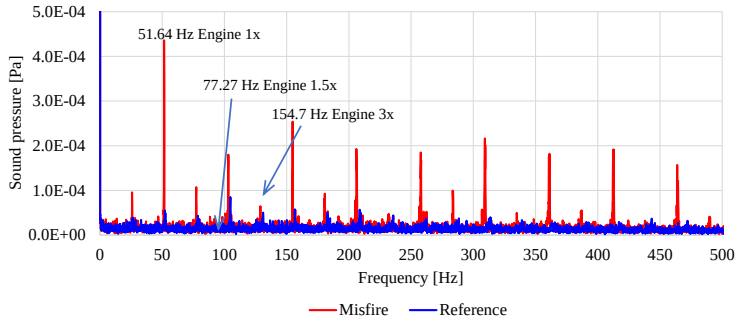

Fig. 12. Microphone's modulation spectrum comparison at 3000 rpm.

method reveals the resonance frequencies without mistake based on excitation and helps to avoid misunderstandings during analysis. The time domain can be transformed into the frequency domain with FFT. The energy content of the microphone signal in terms of frequencies is represented in the spectrum at 3000 rpm motor speed, as shown in Fig. 11. This gives a slight correlation with the fault, though the correlation is even weaker at lower speeds below 3000 rpm. Based on the spectrum, it is difficult to identify the problem. There is a deviation in the frequency range of 1 kHz–10 kHz, due to assumed amplitude modulations. While the operation of the misfire is visible in the spectrum, it is challenging to identify a specific frequency component related to a particular part of the engine. Based on the aforementioned analysis, we reasonably assume that – based on the FFT vs. time analysis as well – that there is amplitude modulation in the signal. Since the FFT vs. time diagram shows that a wide frequency range of the signal is affected, it makes sense to check the modulation spectrum.

The modulation spectrum provides overview of the modulation frequencies across the entire or a selected frequency range. The modulation spectrum shown in Fig. 12 includes the frequency range of 2.8 kHz–5.6 kHz. The envelope low-pass frequency is 1000 Hz, so the frequencies that modulate the signal appear up to 1000 Hz. The analysis reveals that the half-order motor frequency plays a significant role in the modulation. Specifically, the modulation frequency is 25 Hz, which is half of the crankshaft's rotation frequency.

4. Discussion

In this paper, the misfire event in a motor vehicle was studied with vibroacoustic methods. The misfire caused an unbalanced, or more accurately, uneven rotation of the crankshaft. By analyzing the microphone's time-domain signal, one can make a clear distinction between healthy and faulty conditions of the engine. A short frequency calculation analysis showed that the ignition plays a main role in the vibration behavior of both the car body and passenger area. The FFT spectrum also indicates the presence of the failure, similarly to the time-domain signal, but tracking the frequency components in the spectrum does not allow for precise localization of the failure.

The most useful method was the FFT vs. time analysis, where the topological integer and odd-order engine showed increased energy in the faulty condition. The outcome of the modulation spectrum confirmed that there is subharmonic motor order modulation in the spectra. This result allowed us to localize the place of the noise problem inside the car. However, even without advanced analysis, a trained ear could identify that the issue likely originates from the engine.

In summary, with the help of vibroacoustic methods the noise problem could be spotted inside a vehicle. However, with the current measurement points and tools, it is possible to determine in which cylinder the misfire occurs. This could be potentially achieved by placing more acceleration sensors on the car body, for example, on the left front side. Based on the re-

sults, the possible location of the noise problem can be narrowed down; however, the type of the malfunction is not clearly identified.

The reason behind this is that we cannot be sure that only a misfire failure causes the observed acoustic patterns and changes in the spectrograms. It is not the misfire itself, but rather its consequences or, more precisely, the complete absence of the stroke in cylinder 1 (resulting in uneven running of the crankshaft) that determines the vibration behavior of the engine. The shafts are statically and dynamically balanced during manufacturing to account for the moving masses in the crank mechanism, ensuring they do not generate significant radial vibrations. Due to the uneven running of the shaft, torsional vibration occurs, but these were not measured. However, vertical and horizontal vibrations can originate from gas forces and mass forces, although the cylinders were not modified. At this point, the unevenness of the gas forces must be considered, because in the first cylinder only the maximum pressure (2 MPa–3 MPa) ,corresponding to the compression cycle, prevails at the end of the combustion cycle. In contrast, in the other three cylinders, a higher pressure (8 MPa–10 MPa) derived from ignition, is present at the beginning of work cycle.

This difference in cylinder pressure causes abnormal torque behavior, which is why orders with odd numbers and subharmonic orders are present in the result. Practically, the tested engine operates as a 3-cylinder engine where odd orders such as the 1.5th, 3rd, etc., and subharmonics appear. However, despite of this, the four pistons are moving, so integer order numbers (1st, 2nd, 4th, etc.) are also present in the spectrograms. The acoustical pattern of this failure is not unique; other malfunctions that affect crankshaft rotation can trigger the same vibroacoustic behavior. This means that joint analysis alone is not capable to identify the misfire; other non-vibroacoustic measurements are essential for exclusively detecting the problem.

5. Further plans

The low-frequency motor modulation can be linked to psychoacoustical parameters such as fluctuation strength and roughness. These parameters could possibly serve as good indicators of this type of failure, but to justify the relevance of this idea further investigation is necessary. As a continuation of the research, it would be worth to examine how the vibration behavior of the vehicle changes when more than one cylinder is misfiring. Furthermore, we are interested in examining other malfunctions, e.g., valve clearance defect. The ultimate goal is to pinpoint the misfiring cylinder and distinguish this failure mode from other malfunctions using only vibroacoustic tools.

References

1. Babu Devasenapati S., Sugumaran V., Ramachandran K.I. (2010), Misfire identification in a four-stroke four-cylinder petrol engine using decision tree, *Expert Systems with Applications*, **37**(3): 2150–2160, https://doi.org/10.1016/j.eswa.2009.07.061.
2. Brecher C., Gorgels C., Carl C., Brumm M. (2011), Benefit of psychoacoustic analysing methods for gear noise investigation, *Gear Technology*, **28**(5): 49–55.
3. Cavina N., Corti E., Minelli G., Serra G. (2002), Misfire detection based on engine speed time-frequency analysis, *SAE Transactions*, **111**: 1011–1018, http://www.jstor.org/stable/44743127.
4. Delvecchio S., Bonfiglio P., Pompoli F. (2018), Vibro-acoustic condition monitoring of internal combustion engines: A critical review of existing techniques, *Mechanical Systems and Signal Processing*, **99**: 661–683, https://doi.org/10.1016/j.ymssp.2017.06.033.
5. Firmino J.L., Neto J.M., Oliveira A.G., Silva J.C., Mischina K.V., Rodrigues M.C. (2012), Misfire detection of an internal combustion engine based on vibration and acoustic analysis, *Journal of the Brazilian Society of Mechanical Sciences and Engineering*, **43**: 336, https://doi.org/10.1007/s40430-021-03052-y.
6. Szabó J.Z., Dömötör F. (2022), Comparative testing of vibrations in vehicles driven by electric motor and internal combustion engine (ICE), [in:] *Vehicle and Automotive Engineering 4*, Jármai K., Cservenák Á. [Eds.], pp. 871–879, https://doi.org/10.1007/978-3-031-15211-5_72.
7. Turney S. (2022), Skewness. Definition, examples & formula, https://www.scribbr.com/statistics/skewness/ (access: 05.01.2024).
8. Wojnar G., Czech P., Stanik Z. (2011), Use of amplitude estimates and nondimensional discriminants of vibroacoustic signal for detection of operational wear of rolling bearings, *Scientific Journal of Silesian University of Technology. Series Transport*, **72**: 109–114.
9. Wojnar G., Madej H. (2009), Averaged wavelet power spectrum as a method of piston – Skirt clerance detection, *Diagnostyka*, **2**(50): 93–98.
10. Wojnar G., Stanik Z. (2010), Influence of wear of bearings carriageable wheels on acoustics pressure, *Scientific Journal of Silesian University of Technology. Series Transport*, **66**: 117–122.